

# Novel Two-Band Ratiometric Fluorescence Probes with Different Location and Orientation in Phospholipid Membranes

Andrey S. Klymchenko,<sup>1,2</sup> Guy Duportail,<sup>4</sup>

Turan Ozturk,<sup>1</sup> Vasyl G. Pivovarenko,<sup>2</sup>

Yves Mély,<sup>4</sup> and Alexander P. Demchenko<sup>1,3,5</sup>

<sup>1</sup>TUBITAK Research Institute  
for Genetic Engineering and Biotechnology

Gebze-Kocaeli 41470

Turkey

<sup>2</sup>Department of Chemistry

Kyiv National Taras Shevchenko University

01033 Kiev

<sup>3</sup>A.V. Palladin Institute of Biochemistry

9 Leontovicha Street

01030 Kiev

Ukraine

<sup>4</sup>Laboratoire de Pharmacologie et Physicochimie  
des Interactions Cellulaires et Moléculaires

UMR 7034 du CNRS

Faculté de Pharmacie

Université Louis Pasteur

BP 24, 67401 Illkirch

France

## Summary

3-hydroxyflavone (3-HF) derivatives are very attractive fluorescence sensors due to their ability to respond to small changes in their microenvironment via a dramatic alteration of the relative intensities of their two well-separated emission bands. We developed fluorescence probes with locations at different depths and orientations of 3-HF moiety in the phospholipid bilayer, which determine their fluorescence behavior. While the spectral shifts of the probes correlate with their binding site polarity, the intensity ratio is a complex parameter that is also sensitive to the local hydration. We demonstrate that even the deeply located probes sense this hydration effect, which can be modulated by the charge of the lipid heads and is anisotropic with respect to the bilayer plane. Thus the two-band ratiometric fluorescence probes can provide multiparametric information on the properties of lipid membranes at different depths.

## Introduction

Fluorescence microscopy of the living cell is a rapidly developing field of research with countless potentialities [1–3], and the success in visualization of cellular substructures, membranes, and macromolecules provided a strong impulse for further development of this method. One of the very promising prospects that is still poorly explored at the biological membrane level is the possibility of providing the color-changing response to different structural perturbations in cell membranes that can be offered by two-color ratiometric probes [4]. The strong

demand for these probes cannot be satisfied without introduction of new fluorophores and their chemical modifications in order to endow them with the desirable properties. Requirements imposed on these properties are much more stringent than that for the commonly applied probes for fluorescent labeling. In addition to high chemical and photochemical stability and high fluorescence quantum yield, they should provide strong change of color in response to different membrane perturbations. In this sense the common polarity-sensitive [5] and electrochromic [6] dyes have very limited capabilities, as these probes commonly provide the response by shifting one broad band that is present in emission, and the magnitude of the shift is usually smaller than the bandwidth. In order to be sensitive to the two-band ratiometric probe, the dye is required to exhibit an excited-state reaction: isomerization, electronic charge transfer, or proton transfer [7]. In addition, both initial and product forms of the reaction should be present in emission and provide high-intensity and well-separated fluorescence bands. Then, the ratio of intensities of these bands can become a signal of membrane perturbations, which is very attractive for precise measurement and analysis.

There is one family of fluorophores, 3-hydroxyflavones (3-HF), which potentially satisfies these requirements. They exhibit the excited-state intramolecular proton transfer (ESIPT) reaction, which results in two emission bands belonging to normal excited state ( $N^*$ ) and to the photo-tautomer ( $T^*$ ) reaction product [8–12]. The latter is shifted dramatically to longer wavelengths so that the two forms can be easily seen in emission as resolved separate bands. The positions of the two bands and, what is most essential, the ratios of their intensities are very sensitive to different perturbations. Therefore, 3-HF derivatives have found important applications in the studies of reverse micelles [13, 14], phospholipid [15–17] and natural [18] membranes. New strategies have recently been found for improvement of spectroscopic properties of the parent 3-HF chromophore [19, 20]. They allow shifting its absorption and fluorescence spectra to longer wavelengths, increasing the quantum yield and modulating the two-wavelength sensitivity within the desired ranges.

The other unique sensor property of 3-HF chromophore is the ability to report on different properties of environment simultaneously. Its heterocyclic  $\pi$ -electronic system, which provides the strong increase in asymmetry of charge distribution in the excited state, allows the shifts of fluorescence spectra similarly to common solvatochromic and electrochromic dyes; but since the two bands in emission originate from two separate excited states,  $N^*$  and  $T^*$ , with different magnitudes and orientations of their dipole moments [11, 12], the sensitivity of these states to polarity and electric field perturbation of their microenvironment is different. The ESIPT reaction site is strictly localized between 3-hydroxyl and 4-carbonyl groups, which form a hydrogen bond that closes a low-stable five-membered ring [8]. Therefore,

<sup>5</sup>Correspondence: dem@rigeb.gov.tr

this reaction shows extreme sensitivity to intermolecular hydrogen bond perturbations [9] that should have a certain directionality in space. Moreover, because of the asymmetric nature of the chromophore and unidirectional nature of ESIPT reaction, the fluorescence spectra are expected to be sensitive to anisotropic properties of the environment and in particular to electrostatic fields. This is extremely attractive in the studies of different structurally anisotropic systems such as micelles, monolayers, and biological membranes.

Application of these properties cannot be efficient without providing the chromophore the ability of occupying definite location and orientation in the membrane. The most efficient method for the emplacement of the chromophore at the desirable site in the bilayer is the attachment of a positively charged group. This allows its localization at the bilayer interface due to interaction of this group with the negative charge of phosphate groups [21, 22]. Particularly, this can be important for those low-polar chromophores that are intended to protrude deeply into the bilayer [6]. Additional stabilization and orientation of the probe can be achieved by introduction at proper places of aliphatic hydrocarbon chains of different lengths, which make the probe properties close to that of lipids.

In this study, we synthesized novel flavone derivatives containing quaternary ammonium group as an attached positive charge, and hydrocarbon chains at different positions. These modifications are made with strong concern toward maintaining, unchanged, the property of the 3-hydroxyflavones to undergo ESIPT reaction, allowing very sensitive and convenient two-band ratio metric detection in fluorescence.

## Results and Discussion

### Synthesis

In order to introduce a charged group to a 3-hydroxyflavone chromophore from the chromone side, the starting material, 5-chloromethyl-2-hydroxyacetophenone, was prepared (Figure 1). Chloromethylation of 2-hydroxyacetophenone with paraformaldehyde in concentrated HCl at 40°C occurs at the 5 position. The product, which is pure enough for the next step, was obtained in high yield. Applying a common procedure [23], the latter was converted into corresponding chalcone with subsequent oxidative heterocyclization with hydrogen peroxide. Resultant 6-ethoxymethylflavones were transformed into bromomethyl derivatives by heating at 100°C in 62% HBr. The reactions proceed quickly and in good yields. 6-Bromomethyl-3-HF derivatives are very reactive fluorescence labels in which bromine can be easily substituted with amino or mercapto groups. To synthesize the target compounds **F2N8** and **F4N1**, the substitution of bromine was carried out with different tertiary amines.

In order to introduce a positive charge from the opposite side of the flavone chromophore (the phenyl ring), the starting material, 4-[4-(4-pyridyl)piperazino]benzaldehyde, was prepared in two steps from 4-chloropyridine and 1-phenylpiperazine, followed by introduction of the formyl group into the intermediate, 1-phenyl-4-(4-pyridyl)piperazine (Figure 1). Both steps proceeded

with relatively high yields. Then, the aldehyde was condensed with 2'-hydroxyacetophenone, and the resultant chalcone was transformed into corresponding flavone. Finally, the obtained flavone was transformed into corresponding zwitterionic compound **PPZ** by treating with 1,3-propanesultone. It should be noted that **PPZ**, unlike all the other products, is less soluble in common organic solvents except DMSO.

### Absorption and Fluorescence Properties in Neat Solvents

All the new probes display two bands in emission spectra. Thus, they retain the property of being able to undergo ESIPT, which is manifested by the presence of two N\* and T\* emission bands, but the relative intensities of these bands exhibit broad variations (Figure 2). Flavone probes **F2N8** and **F4N1**, which possess the positively charged group attached to chromone unit, demonstrate almost identical absorption and fluorescence spectra in various neat solvents (Table 1). However, when compared with the parent flavone **F**, they show both absorption and fluorescence spectra shifted to longer wavelengths together with significant increase of relative intensity of the N\* band. In contrast, flavone **PPZ** shows considerable blue shifts in the spectra along with a decrease of the relative intensity of N\* band (Figure 2; Table 1). These differences can be attributed to an effect of proximity to the chromophore of positive charge, which, interacting electrostatically with 3-HF moiety, either stabilizes (**F2N8**, **F4N1**) or destabilizes (**PPZ**) its N\*-excited state. This phenomenon was recently studied in detail for a series of charged and uncharged 3-HF derivatives in the solvents of different dielectric properties [24]. It was found that the intensity ratio of N\* and T\* bands can exhibit dramatic electrochromic modulation (internal Stark effect), and the dielectric screening of the proximal charge by the dipolar molecules or ions decreases the effect.

Similarly to the parent flavone **F**, all the novel flavones demonstrate strong sensitivity to the polarity of their environment. Increase of solvent polarity for all the probes results in gradual red shift of the N\* band, which is accompanied by dramatic increase of fluorescence intensity ratio between N\* and T\* bands, I<sub>N</sub>/I<sub>T</sub> (Figure 2). This is typical for 3-HF derivatives possessing 4'-dialkylamino substituent in the phenyl ring. The presence of the donor group induces a large dipole moment in the excited N\* state, making it strongly solvatochromic[10-12].

### Binding of the Probes to Phospholipid Membranes

Binding to lipid vesicles was monitored by the change of fluorescence intensity in the presence of increasing lipid concentrations. A strong, up to 100-fold, increase of intensity upon binding to large unilamellar vesicles composed of dioleoyl phosphatidylcholine (DOPC) is observed for all the probes considered (Figure 3). With the probe concentration of 1 μM, the binding appears to be quite efficient in the cases of **F**, **F2N8**, and **F4N1**, since the plateau is reached at a lipid concentration of 200 μM. **PPZ** seems to be less prone to binding to vesicles since the plateau is approached only at 400–600

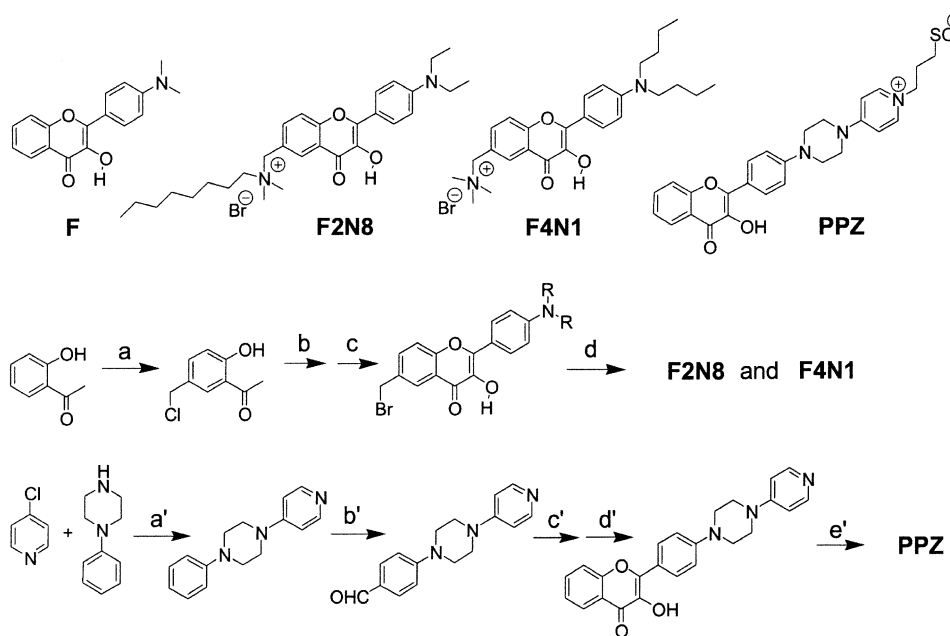


Figure 1. Chemical Structures of the Studied Probes and Pathways of Synthesis for F2N8, F4N1, and PPZ

R =  $\text{C}_2\text{H}_5$  or  $n\text{-C}_4\text{H}_9$ ; (a),  $\text{CH}_2\text{O}$ ,  $\text{HCl}$ ,  $35^\circ\text{C}$ ; (b), 4-dialkylaminobenzaldehyde,  $\text{OH}^-$ ,  $\text{EtOH}$ ; (c),  $\text{H}_2\text{O}_2$ ,  $\text{OH}^-$ ,  $\text{EtOH}$ ,  $0^\circ\text{C}$ ; (d),  $\text{N,N-dimethyloctylamine}$  or  $\text{trimethylamine}$ ,  $\text{EtOH}$ ,  $t^\circ$ ; (a'), diisopropylethylamine, nitrobenzene,  $200^\circ\text{C}$ ; (b'), dimethylformamide,  $\text{POCl}_3$ ,  $60^\circ\text{C}$ ; (c'), 2-hydroxyacetophenone,  $\text{OH}^-$ ,  $\text{EtOH}$ ; (d'),  $\text{H}_2\text{O}_2$ ,  $\text{OH}^-$ ,  $\text{EtOH}$ ,  $0^\circ\text{C}$ ; (e'), 1,3-propanesultone,  $\text{DMF}$ ,  $100^\circ\text{C}$ .

$\mu\text{M}$ . The probe and DOPC concentrations for subsequent quenching experiments were selected according to these data.

#### Location of the Probes in Phospholipid Bilayer

In order to provide information on the probe location in the bilayer, fluorescence quenching experiments of these probes by spin-labeled lipids were performed by using the parallax method [25, 26]. Their fluorescence was quenched with shallow (TempoPC), medium (5-SLPC), or deep (12-SLPC) nitroxide-labeled phosphatidylcholines in DOPC vesicles prepared by either ethanol or octylglucoside dilution. The relative amount of fluorescence quenching obtained by the introduction of different quenchers was employed to calculate fluorophore depth using the parallax equation (see Experimental Procedures). The location of the dyes was expressed as  $Z_{\text{ct}}$ , which corresponds to the distance of the fluorophore from the center of the lipid bilayer (more precisely, the distance from the border between the two leaflets to the center of the fluorophore). The quenching experiments with the vesicles obtained by ethanol dilution method were repeated three times. As these vesicles appeared to have a dimension corresponding to large unilamellar vesicles, namely  $0.12 \mu\text{m}$ , this series of experiments was emphasized. For comparison one set of quenching experiments was performed with vesicles obtained by octylglucoside dilution. According to their dimension, these vesicles are probably multilamellar, and despite more scattered quenching data, the results remained coherent with those obtained with unilamellar vesicles (Table 2).

According to these data, the probes F and F2N8 locate

at  $16 \pm 1$  and  $15 \pm 1 \text{ \AA}$ , respectively, from the center of the bilayer. This location is at the level of the ester groups and glycerol residues of phospholipids [27] and is somewhat deeper than the location of the most common dyes with charged groups, like rhodamine B, fluorescein, and ANS ( $16.5\text{--}18.5 \text{ \AA}$ ) [28]. Meanwhile, chromophores of probes F4N1 and PPZ locate much deeper in the region of hydrocarbon chains at  $10 \pm 1$  and  $7 \pm 1.5 \text{ \AA}$  from the center, respectively. These quite contrasting results were expected considering the chemical structures of the probes. Probe F is an uncharged and relatively hydrophobic molecule; therefore, it can locate at any depth inside the low-polar bilayer interface. However, the presence of two polar groups, 3-hydroxyl and 4-carbonyl, which tend to form intermolecular hydrogen bonds with water and polar groups of lipids, can be sufficient for its location preferentially near the interface. In an analogous case of another hydrophobic aromatic molecule, 9-methylanthracene, which shows deep location in the bilayer, an introduction of hydroxyl group results in translocation of the chromophore next to the interface [29]. F2N8 is a charged molecule with a quaternary ammonium acting as an anchor at the interface [30]. The presence of strongly hydrophobic octyl hydrocarbon chain, probably aligned along the fatty acid chains of the phospholipids, imposes on the fluorophore an oblique orientation exposing 3-hydroxyl and 4-carbonyl groups to the membrane interface. This results in apparent similarity in the location of probes F and F2N8. However, F2N8 seems to be located more precisely than F, as can be seen from the quenching data (Table 2). Indeed, the medium nitroxide-PC quenches F and F2N8 with the same efficiency, while shallow and deep quenchers affect much stronger probe F, which is probably due

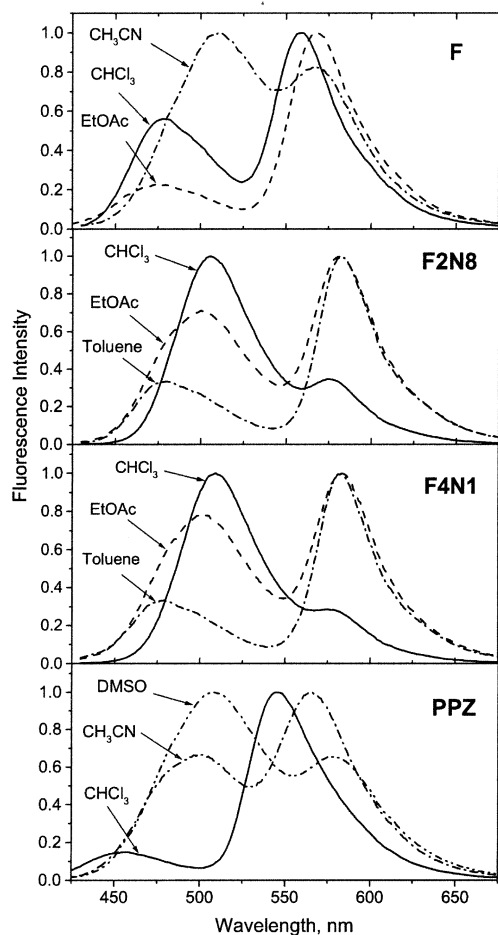


Figure 2. Fluorescence Spectra of the Studied Probes in Different Solvents: Excitation Wavelength 410 nm

to its broader distribution to deep and shallow areas. In contrast to **F2N8**, probe **F4N1** contains a smaller polar trimethylammonium group and a large hydrophobic 4'-dibutylamino substituent at the opposite side of the flavone chromophore. Therefore, it has to penetrate deeply into the hydrophobic core of the bilayer and attain its vertical or almost vertical orientation with respect to the bilayer plane. The ammonium groups of **F2N8** and **F4N1** should be fixed at almost the same positions close to the phosphate groups of the membrane phospholipids. Taking this into account, the observed 5 Å difference in the depth of the chromophores (the size  $\approx$ 10 Å) in the phospholipid layer can only be explained by their almost perpendicular orientations with respect to each other in the lipid bilayer. The long hydrophobic spacer separating the zwitterionic polar headgroup and the flavone moiety probably imposes the observed deep location of probe **PPZ**. However, its orientation can be more flexible because the flavone moiety of this probe is not as hydrophobic as in probe **F4N1**.

These results allow us to schematize the location of the different probes in Figure 4. The important peculiarities in location of the probes' ESIPT reaction site (3-hydroxyl and 4-carbonyl groups) should be noted.

While in the case of **F** and **F2N8**, it locates on the level of  $sn_2$  carbonyls of phospholipids, for **F4N1** and **PPZ** it is close to the deeper  $sn_1$  carbonyls (Figure 4).

### Fluorescence Behavior of Probes in Phospholipid Vesicles

#### *Effect of Incorporation into Vesicles*

Incorporation of the probes into vesicles results in a very strong increase of fluorescence intensity (Figure 3), which is in line with their much higher quantum yields in vesicles with respect to water (Table 1). Only for **PPZ** is this difference in quantum yields lower. The quenching of 3-HF fluorescence in water is well known [9]. The screening from bulk water together with restriction in mobility of the environment are probably the two major factors responsible for the increase in probability of radiative transition from both  $N^*$  and  $T^*$  states. Importantly, for all the studied probes, the quantum yield in vesicles is much higher than in different organic solvents, which suggests that the restriction of mobility is an important factor.

For all the studied probes, the excitation spectra in phospholipid vesicles match closely the absorption spectra and do not differ considerably when recorded at  $N^*$  or  $T^*$  emission band maxima. This result, which is similar to that observed in neat solvents, allows us to rule out the presence of the anion form in emission and consider the two bands as originating from the same ground-state species.

Fluorescence spectra of probe **F** in the studied PC vesicles (Figure 5) are similar to those obtained in aprotic solvents and correspond to the solvent polarity range between ethyl acetate and acetonitrile (Figure 2). This is in correspondence with the data on preferable location of the dye at the level of the glycerol moiety observed by the parallax method. Surprisingly, the differences in fluorescence spectra between the probe **F** and the charged probe **F2N8** in DOPC and EYPC (egg yolk phosphatidylcholine) vesicles are less pronounced than those observed in neat organic solvents. While in these solvents (see Figure 2) the  $N^*$  band of probe **F2N8** is substantially red shifted (by 26 nm in ethyl acetate), in PC vesicles its position is almost the same as that of probe **F** (Figure 5). A similar observation is made for fluorescence intensity ratio,  $I_{N^*}/I_{T^*}$  (Table 1). For flavone **F2N8**, this ratio is higher by approximately three times in ethyl acetate as compared to **F**, while in DOPC vesicles the difference is by 1.3 times only. The same tendency is observed for probes **F4N1** and **PPZ**. The absorption spectra for probes **F**, **F2N8**, **F4N1**, and **PPZ** in the PC vesicles are very similar to those obtained in neat solvents (Table 1); therefore, the origin of these variations should be in the excited-state electrostatic influence of positively charged substituent, which becomes screened on incorporation into the bilayer. Most probably, it is the screening of positively charged groups of probes **F2N8**, **F4N1**, and **PPZ** by the negatively charged phospholipid phosphate headgroups.

It should also be noted that the fluorescence spectra of the studied probes do not differ in the range of the lipid concentration 25–800  $\mu$ M (data not shown). The only exception is probe **PPZ** since its fluorescence spec-

Table 1. Spectroscopic Properties of Flavone Probes in Solvents and Phospholipid Vesicles

Probe	Solvent/Vesicles	$\lambda_{\max}^{\text{abs}}$	$\lambda_{\max}^{N^*}$	$\lambda_{\max}^{T^*}$	$I_{N^*}/I_T$	$\phi$
F	Ethyl acetate	394	475	567	0.229	0.03
	Acetonitrile	395	509	569	1.20	0.09 <sup>a</sup>
	Water	410	554	—	—	0.003
	DOPC vesicles	406	518	569	0.862	0.42
	DOPG vesicles	409	515	560 <sup>b</sup>	1.089	0.42
	EYPC vesicles	403 <sup>c</sup>	511	569	0.698	—
	EYPG vesicles	404 <sup>c</sup>	510	565	0.866	—
F2N8	Ethyl acetate	413	501	581	0.709	0.13
	Water	423	560	—	—	$\leq 0.002$
	DOPC vesicles	421	515	573	1.111	0.58
	DOPG vesicles	424	510	572	1.351	0.59
	EYPC vesicles	421 <sup>c</sup>	511	574	1.125	—
	EYPG vesicles	422 <sup>c</sup>	510	573	1.292	—
F4N1	Ethyl acetate	413	501	581	0.783	0.17
	Water	408	550	—	—	$\leq 0.002$
	DOPC vesicles	421	496	573	1.515	0.45
	DOPG vesicles	423	500	571	1.898	0.44
	EYPC vesicles	422 <sup>c</sup>	500	573	1.521	—
	EYPG vesicles	424 <sup>c</sup>	500	571	1.669	—
PPZ	Acetonitrile	380	499	565	0.669	0.075
	Water	386	538	—	—	0.03
	DOPC vesicles	385	518	570	0.631	0.25
	DOPG vesicles	394	520	569	0.552	0.33
	EYPC vesicles	394 <sup>c</sup>	520 <sup>c</sup>	572	0.480	—
	EYPG vesicles	396 <sup>c</sup>	519 <sup>c</sup>	568	0.490	—

$\lambda_{\max}^{\text{abs}}$ , position of absorption maxima;  $\lambda_{\max}^{N^*}$  and  $\lambda_{\max}^{T^*}$ , position of fluorescence maxima of  $N^*$  and  $T^*$  forms.  $\phi$  is the fluorescence quantum yield.

<sup>a</sup> Reference [12].

<sup>b</sup> The band appears as a shoulder.

<sup>c</sup> The values correspond to excitation maxima recorded at the  $T^*$  band peak.

tra at lipid concentrations below 600  $\mu\text{M}$  contain some contribution from bulk solution, where this probe exhibits a nonnegligible quantum yield.

#### Insensitivity to Variation in Fatty Acid Residues

The parent uncharged probe F shows lower relative intensity of  $N^*$  band ( $I_{N^*}/I_T$ ) in EYPC as compared to DOPC vesicles, demonstrating the decreased polarity of its

surrounding (Figure 5; Table 1). This can be explained by redistribution of the probe to greater depths in the EYPC bilayer, the hydrophobic region of which displays broader structural heterogeneity due to the larger variety of fatty acid species. The same is observed with probe PPZ, which can exhibit broader distribution of locations due to long distance between the chromophore and the charged group and lower hydrophobicity of 3-HF moiety. Meanwhile, this effect is absent for F2N8 and F4N1 (Figure 5; Table 1). This can be a result of their much more precise location in a layer 10–15 Å from the bilayer center, the properties of which do not depend significantly on the structure of phospholipid hydrocarbon chains. The same regularity is observed in negatively charged egg yolk phosphatidylglycerol (EYPG) with respect to dioleoyl phosphatidylglycerol (DOPG) vesicles: F2N8 and F4N1 compared to F and PPZ show much smaller decrease in  $I_{N^*}/I_T$  ratio (Figure 5; Table 1). This allows for probes F2N8 and F4N1, avoiding the effect of the fatty acid composition and focusing the analysis on the effects of polarity, electrostatics, and hydrogen bonding.

#### Depth-Dependent Differences in Spectra

While in neat solvents the spectra of probes F4N1 and F2N8 are similar (Figure 2), they exhibit significant differences in all studied vesicles (Figure 5). The  $N^*$  band of F4N1 being blue shifted by 10–19 nm (dependent on the lipid) exhibits a dramatic 1.3- to 1.4-fold increase of relative intensity ( $I_{N^*}/I_T$ ) with no essential differences in

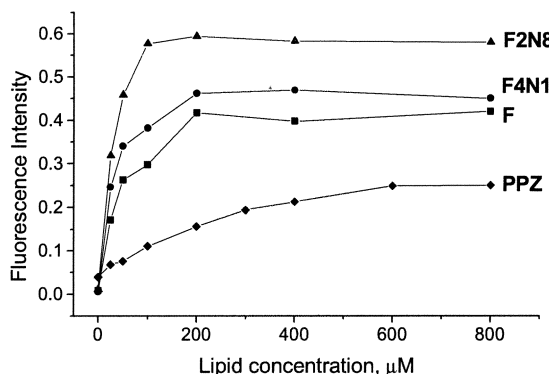


Figure 3. Dependence of Fluorescence Intensity of Flavone Probes at Concentration 1  $\mu\text{M}$  in LUV Vesicles on DOPC Concentration  
The excitation wavelength 400 nm: the integral fluorescence emission intensity was obtained from the area under the spectra (in wavelength scale). The results were normalized with the account of quantum yields of the probes in 800  $\mu\text{M}$  DOPC vesicles.

Table 2. Quenching of 3-Hydroxyflavone Probes by Nitroxide-Labeled Lipids

Probe	Experiment	$F_{tc}/F_0$	$F_s/F_0$	$F_{12}/F_0$	$Z_{cf}, \text{Å}$	$\langle Z_{cf} \rangle, \text{Å}$
F	E1	0.49	0.495	0.55	15.9	16.0
	E2	0.47	0.485	0.53	16.1	
	E3	0.50	0.50	0.57	15.8	
	OG	0.49	0.49	0.52	15.8	
F2N8	E1	0.515	0.49	0.56	15.3	15.0
	E2	0.53	0.49	0.59	15.0	
	E3	0.53	0.475	0.61	14.7	
	OG	0.55	0.54	0.59	15.6	
F4N1	E1	0.535	0.45	0.49	9.9	10.0
	E2	0.50	0.41	0.45	10.1	
	E2	0.56	0.43	0.46	9.8	
	OG	0.67	0.51	0.58	10.5	
PPZ	E1	0.64	0.54	0.49	7.8	7.0
	E2	0.58	0.53	0.46	7.3	
	F3	0.60	0.49	0.39	6.3	
	OG	0.87?	0.47	0.40	7.1	

$Z_{cf}$  is the distance between the middle of the bilayer and the chromophore center for each individual type of preparation (OG refers to the vesicles obtained by octylglucoside dilution);  $\langle Z_{cf} \rangle$  is the average of the three  $Z_{cf}$  values obtained with unilamellar vesicles. The error is probably higher than the one that could be estimated from the deviations from the average and is estimated around  $\pm 1 \text{ \AA}$ , even more in the case of PPZ ( $\pm 1.5 \text{ \AA}$ ).  $F_{tc}/F_0$ ,  $F_s/F_0$ , and  $F_{12}/F_0$  are the values of fluorescence quenching ratios in vesicles containing 15 mol% TempoPC, 5-SLPC, or 12-SLPC, respectively, to DOPC vesicles lacking nitroxide-labeled lipid.

absorption spectra (Table 1). The shift to the blue of the  $N^*$  band for 3-HF derivatives always indicates the decrease of polarity of the chromophore surrounding [10, 11], and this is in line with results of the parallax measurements suggesting the deeper location of F4N1 in the bilayer. What then is the origin of substantial increase of the  $I_N/I_T$  ratio, which is the opposite of the expected polarity effect?

A reasonable explanation could be that the  $N^*$  band position and the  $I_N/I_T$  ratio of the 3-HF probe characterize different properties of the microenvironment. The  $N^*$  band position is sensitive to the polarity of the probe surrounding, with resolution comparable to the size of the  $N^*$ -excited state dipole, ca. 10 Å. Meanwhile, the  $I_N/I_T$  ratio is directly connected with the energetic and

kinetic variables of ESIPT reaction between the proximal 3-hydroxyl and 4-carbonyl groups and, therefore, can report on perturbation of this reaction at the distance of a single hydrogen bond [8]. Since the ESIPT reaction center for probe F4N1 is estimated to locate on the level of  $sn_1$  carbonyl (Figure 4), the water molecules bound at this level [30] may provide this perturbation by intermolecular hydrogen bonding, decreasing the proton transfer efficiency. This result demonstrates that the 3-HF probes can provide an extremely sensitive response to the changes in properties of their binding sites in membrane, and this response is multiparametric.

#### Sensitivity to the Surface Charge

Comparative studies were performed on LUV composed of anionic DOPG and EYPG with respect to neutral

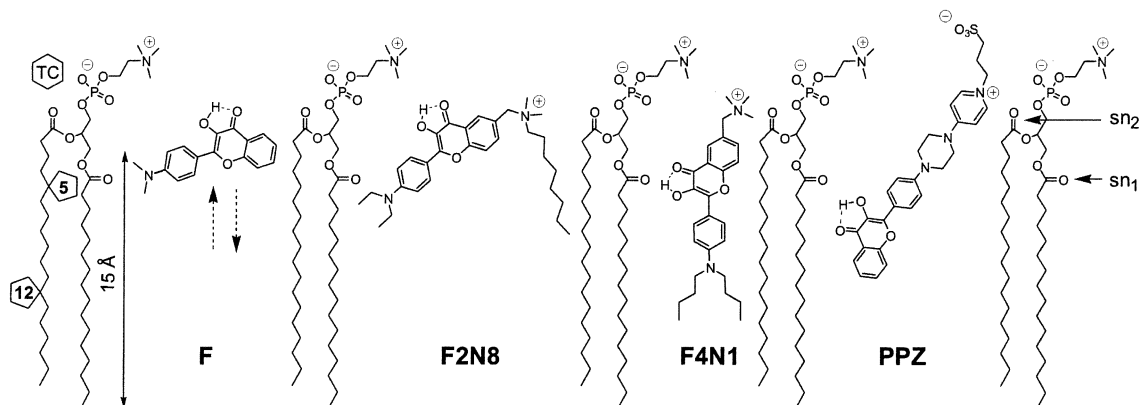


Figure 4. Estimated Location of the Studied Probes in DOPC Lipid Membranes

Location of phospholipid functional groups is based on the study of Wiener and White [27]. Positions of  $sn_1$  and  $sn_2$  carbonyls are indicated by horizontal arrows. Dashed vertical arrows indicate the possibility of relocation of probe F at various depths. Location of nitroxide paramagnetic quenchers is shown as five-/six-membered rings on the left margin.

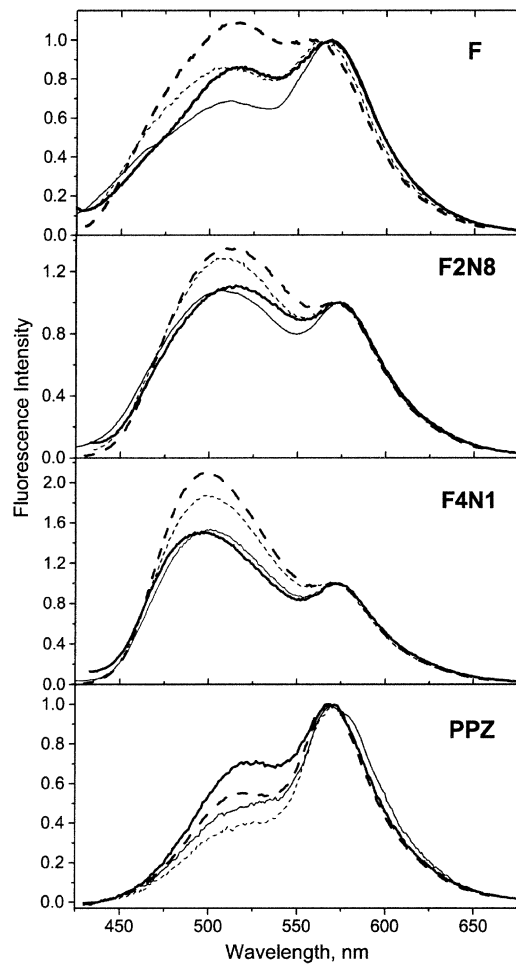


Figure 5. Fluorescence Spectra of the Studied Probes in LUV Vesicles Composed of Different Lipids

DOPC, thick solid line; DOPG, thick dashed line; EYPC, thin solid line; and EYPG, thin dashed line. Concentration of probes was 1  $\mu\text{M}$  and that of lipids 200  $\mu\text{M}$  for F, F2N8, and F4N1 or 800  $\mu\text{M}$  for PPZ. Excitation wavelength, 400 nm. 15 mM HEPES buffer, pH 7.4.

DOPC and EYPC lipids. For probe F2N8, the response is similar to that of probe F (Figure 5), which is in line with their locations at the same depths (Figure 4). The presence of the negative charge on the head groups of DOPG and EYPG lipids results in increase of  $I_N/I_T$  ratio without any considerable spectral shifts of emission bands (Table 1). This result was shown previously with probe F [17], and its observation for more precisely located F2N8 signifies that it is not the translocation of flavone fluorophore, which responds to variations of the surface charge. Probe F4N1, with a significantly deeper location and a more vertical orientation in the membrane, also shows an increase in the  $I_N/I_T$  ratio (Table 1). The spectra obtained with the other deeply located but oppositely oriented probe, PPZ, clearly show a reversal of this effect, i.e., the increase of the negative charge results in the decrease of the  $I_N/I_T$  ratio (Figure 5). The absence of effects of surface charge on positions of absorption and emission spectra of all studied probes (Table 1) shows that these perturbations influence not the whole  $\pi$ -electronic system but some specific inter-

actions at the ESIPT reaction site of the probes. As it was previously proposed for probe F [17], they are connected with the increased hydration of this site in EYPG as compared to EYPC vesicles. For probes F and F2N8, this probably occurs on the level of  $\text{sn}_2$  carbonyl and phosphate groups, while for the deeper located probes F4N1 and PPZ, the hydration site may be located at the level of  $\text{sn}_1$  carbonyls (Figure 4). The deep penetration of water molecules inside the bilayer is a known fact that was established in experiment [30, 31] and confirmed in molecular dynamics simulations [32–34]. The observed opposite effect for PPZ (in comparison with other probes) suggests that all the probes are able to sense the differences in anisotropic properties of the bilayer, which may be connected with oriented dipoles of trapped water molecules.

### Significance

Introduction and development of two-band ratiometric probes is an important breakthrough that should expand enormously the possibilities of fluorescence spectroscopy and microscopy, including the image recording in real color. The new 3-hydroxyflavone derivatives offer unique possibilities in this respect by providing observation of two emission bands, blue-green (at about 500 nm) and yellow-red (at about 600 nm), the spectral positions and relative intensities of which are strongly sensitive to the properties of their microenvironment. Because variations of these properties occur at atomic distances, this sensitivity cannot be applied in full without providing their definite location and orientation in the bilayer. Solution of this problem is presented in the present work. A family of advanced probes has been synthesized which retain all major properties of 3-HF, such as two bands in emission spectra and the dramatic solvent-dependent variations of their intensity ratio. On incorporation into phospholipid vesicles, their well-resolved two emission bands are maintained, and moreover, the fluorescence quantum yields are greatly increased. Dependent on the probe structure, their 3-HF chromophores can locate at different depths and in different orientations.

We show that the two-band fluorescent 3-HF probes inserted into the membrane bilayer allow for obtaining several parameters that characterize the properties of their location sites simultaneously. Similarly to common polarity-sensitive dyes, the shifts of their two emission bands are correlated with polarity of their environment. The intensity ratio of these bands in addition to polarity effects is sensitive to specific interactions that affect ESIPT reaction, and in particular, to intermolecular hydrogen bonding. This provides the possibility of characterizing the hydration of probe binding sites in membranes. Because of unidirectional character of ESIPT reaction, anisotropic properties of probe location sites can also be revealed. We are on the beginning steps of exploration of these unique possibilities.

### Experimental Procedures

#### General Methods

Melting points of the synthesized compounds were determined on a Büchi 512 melting point apparatus and presented as uncorrected

values. Microanalyses were performed with a Carlo Erba 1106 Elemental Analyzer. Proton NMR spectra were recorded at 200 MHz on a JEOL PMX 270 MHz spectrometer. Tetramethylsilane (TMS) was used as an internal standard in all NMR spectra run in  $\text{CDCl}_3$  or  $\text{DMSO}-d_6$ . Mass spectra were recorded on a Kratos MS-25 mass spectrometer using EI or FAB methods. All column chromatography was performed on silica gel (Merck, Kieselgel 60H, Art 7736). Absorption spectra were performed on Cary 3 Bio (Varian) spectrophotometer. Fluorescence spectra in solvents were recorded on Quanta Master (PTI) and those in vesicles on SLM 48000 (SLM-Aminco) spectrofluorometers.

#### Chemicals

All the solvents used for absorption and fluorescence measurements were of spectroscopic grade purchased from Aldrich and Fluka Chemical Co. Acetonitrile and ethyl acetate were additionally dried over phosphorus pentoxide and sodium sulfate, respectively, with subsequent distillation. Dioleoyl and egg yolk phospholipids and octylglucoside were purchased from Sigma Chemical Co. TempoPC, 5-SLPC, and 12-SLPC were purchased from Avanti Polar Lipids. The concentration of phospholipids stock solutions in chloroform was determined by dry weight. The nitroxide content of nitroxide-labeled lipids was calculated using the electron spin resonance integrated spectra of corresponding diluted stock solutions in chloroform by comparing with a tempocholine reference solution in the same solvent.

#### Synthesis of Probes

##### 4'-Dimethylamino-3-Hydroxyflavone (F)

4'-dimethylamino-3-hydroxyflavone (F) was synthesized and purified as described elsewhere [12].

##### 5-Chloromethyl-2-Hydroxyacetophenone

A suspension of 1 ml of 2-hydroxyacetophenone (Aldrich) and 0.27 g of paraformaldehyde in 5 ml of concentrated hydrochloric acid was stirred at 35°C for 4–5 hr until the formation of yellow precipitate, which was filtered and washed thoroughly with water. The precipitate was dried and washed with minimum amount of methanol. Yield 60%; mp 78°C–81°C;  $^1\text{H}$  NMR (200 MHz,  $\text{CDCl}_3$ ) 2.64 (3H, s), 4.56 (2H, s), 6.97 (1H, d,  $J$  8 Hz), 7.49 (1H, dd,  $J$  8.6 Hz, 2.1 Hz), 7.73 (1H, d,  $J$  2.1 Hz), 12.315 (1H, s); Anal. Calcd. for  $\text{C}_9\text{H}_9\text{ClO}_2$  C 58.55%, H 4.91%; found C 58.74%, H 4.99%.

##### 6-Ethoxymethyl-4'-N,N-Diethylamino-3-Hydroxyflavone

1 g of 5-chloromethyl-2-hydroxyacetophenone was dissolved in 10 ml of ethanol. The solution was treated with 0.87 g of sodium hydroxide in 10 ml of water, and the mixture was refluxed for 30 min until it became homogeneous. To the resultant solution, 1.15 g of 4'-N,N-diethylaminobenzaldehyde (Aldrich) was added. The mixture was stirred for 8 hr and then left for 3 days. The red solution of sodium salt of 6-ethoxyethylamino-4'-diethylamino-2-hydroxychalcone was cooled on an ice bath and treated with 3.3 ml of 30% hydrogen peroxide while stirring. The reaction was controlled by TLC (Thin Layer Chromatography) with chloroform:methanol = 9:1 as mobile phase. The solution of the product was neutralized by acetic acid, and the precipitate was filtered and purified by column chromatography on silica gel (hexane:dichloromethane = 8:2). Yield, 34%; mp, 132°C;  $^1\text{H}$  NMR (200 MHz,  $\text{CDCl}_3$ ) 1.19–1.3 (3H and 6H, two t), 3.45 (4H, q,  $J$  7.14 Hz), 3.575 (2H,  $J$  7.16 Hz), 4.61 (2H, s), 6.775 (2H, d,  $J$  9.04 Hz), 6.89 (1H, s), 7.54 (1H, d,  $J$  8.68), 7.685 (1H, dd,  $J$  8.68 Hz; 1.78 Hz), 8.15–8.2 (1H+2H, two d); MS (EI) m/z 367.1 ( $M^+$ ), 352.1, 338.1, 322.1, 307.1, 294.1, 279.1, 161.5, 133.0; Anal. Calcd. for  $\text{C}_{22}\text{H}_{25}\text{NO}_4$  C 71.92%, H 6.86%, N 3.81%; found C 71.63%, H 6.84%, N 3.72%.

##### 6-Bromomethyl-4'-N,N-Diethylamino-3-Hydroxyflavone

6-ethoxymethyl-4'-N,N-diethylamino-3-hydroxyflavone in 63% hydrobromic acid was heated on an oil bath at 100°C for 3 hr. The cooled solution was neutralized with 10% sodium carbonate, and the resultant precipitate was filtered and washed with water. Yield, 95%; mp, 132°C–133°C;  $^1\text{H}$  NMR (200 MHz,  $\text{CDCl}_3$ ) 1.23 (6H, t,  $J$  7.0 Hz), 3.45 (4H, q,  $J$  7.0 Hz), 4.60 (2H, s), 6.76 (2H, d,  $J$  8.50), 6.87 (1H, s), 7.54 (1H, d,  $J$  8.73), 7.68 (1H, dd,  $J$  8.73 Hz; 1.93 Hz), 8.16 (2H, d,  $J$  8.50), 8.215 (1H, d,  $J$  1.93); MS (EI) m/z 403.1 ( $M^++2$ ), 401.1 ( $M^+$ ), 388.0, 322.1, 314.0, 278.1, 153.5, 133.0.

##### N-[(4'-N,N-Diethylamino)-3-Hydroxy-6-Flavonyl]Methyl-N,N-Dimethyloctyl Ammonium Bromide (F2N8)

A mixture of 30 mg of 6-bromomethyl-4'-N,N-diethylamino-3-hydroxyflavone and 20 mg of N,N-dimethyloctylamine (Aldrich) was dissolved in 3 ml of dry tetrahydrofuran. After stirring for 4 hr, the formed precipitate was filtered and washed with cold tetrahydrofuran. Yield, 60%; mp, 153°C–154°C; UV max in acetonitrile 417 nm,  $\epsilon$  = 34,000  $\text{l} \times \text{mol}^{-1} \times \text{cm}^{-1}$ ;  $^1\text{H}$  NMR (200 MHz,  $\text{CDCl}_3$ ) 0.85 (3H, t,  $J$  5.80), 1.2–1.4 (18H, multiplet), 3.33 (6H, s), 3.4–3.6 (6H, multiplet), 5.28 (2H, s), 6.7–7.0 (3H, multiplet), 7.59 (1H, d,  $J$  8.44), 8.15 (2H, d,  $J$  8.17), 8.22 (1H, s), 8.35 (1H, d,  $J$  8.44); MS (FAB) m/z 479.2 ( $M^+$ ), 322.1, 239.6, 154.0.

##### 6-Bromomethyl-4'-N,N-Dibutylamino-3-Hydroxyflavone

This compound was prepared as 6-bromomethyl-4'-N,N-diethylamino-3-hydroxyflavone in two steps starting from 5-chloromethyl-2-hydroxyacetophenone and 4-dibutylaminobenzaldehyde (prepared in two steps from aniline and n-butyl iodide and further formylation). Resulted ethoxyflavone was transformed to bromomethyl as described above. Mp, 199°C–200°C;  $^1\text{H}$  NMR (200 MHz,  $\text{CDCl}_3$ ) 0.97 (6H, t,  $J$  7.2 Hz), 1.38 (4H, m,  $J$  7.2 Hz), 1.62 (4H, m,  $J$  7.2 Hz), 3.36 (4H, t,  $J$  7.2 Hz), 4.60 (2H, s), 6.73 (2H, d,  $J$  9.1 Hz), 7.53 (1H, d,  $J$  8.7 Hz), 7.68 (1H, dd,  $J$  8.7, 2.0 Hz), 8.14 (2H, d,  $J$  9.1 Hz), 8.21 (1H, d,  $J$  2.0 Hz); MS (FAB) m/z 459.1 ( $M^++2$ ), 457.1 ( $M^+$ ), 232.

##### N-[(4'-N,N-Dibutylamino)-3-Hydroxy-6-Flavonyl]Methyl-N,N,N-Trimethyl Ammonium Bromide (F4N1)

A solution of 0.1 g of 6-bromomethyl-4'-N,N-dibutylamino-3-hydroxyflavone, 0.1 g of trimethylamine hydrochloride, and 0.11 ml of ethyldiisopropylamine in ethanol was boiled for 5 hr. The product was isolated after the solvent was evaporated on a rotary evaporator, and crystallized from dichloromethane/hexane mixture. Hygroscopic crystals were obtained. UV max in acetonitrile 417 nm,  $\epsilon$  = 32,000  $\text{l} \times \text{mol}^{-1} \times \text{cm}^{-1}$ ;  $^1\text{H}$  NMR (200 MHz,  $\text{CDCl}_3$ ) 0.97 (6H, t,  $J$  7.2 Hz), 1.39 (4H, m), 1.64 (4H, m), 3.34 (9H, s), 3.4–3.6 (6H, multiplet), 5.27 (2H, s), 6.7–7.0 (3H, multiplet), 7.59 (1H, d,  $J$  8.4), 8.15 (2H, d,  $J$  8.1), 8.22 (1H, s), 8.35 (1H, d,  $J$  8.4); MS (FAB) m/z 437.2 ( $M^+$ ), 378.2.

##### 1-Phenyl-4-(4-Pyridyl)Piperazine

A mixture of 4 g of 4-chloropyridine hydrochloride (Aldrich), 4 ml of 1-phenylpiperazine (Aldrich), and 14 ml of ethyldiisopropylamine (Fluka) in 20 ml of nitrobenzene (Aldrich) was heated with stirring for 4 hr at 200°C. The resultant solution was concentrated on a rotary evaporator and then water was added. The precipitate was filtered and washed with water and hexane. Crystallized from toluene/hexane = 1/1, yield 60%; mp, 163°C. This compound was used in the next step without any further characterization.

##### 4-[4-(4-Pyridyl)Piperazino]Benzaldehyde

To 8 ml of dry dimethylformamide (DMF), 2.4 ml of  $\text{POCl}_3$  was added dropwise with stirring and cooling on ice bath. To the solution, 2 g of 1-phenyl-4-(4-pyridyl)piperazine was added, and the mixture was heated at 60°C for 1 hr, then cooled and poured into ice bath. The precipitate formed after neutralization with sodium carbonate was filtered and washed with water and hexane. It was crystallized from toluene; yield, 89.5%; mp, 119°C–120°C;  $^1\text{H}$  NMR (200 MHz,  $\text{CDCl}_3$ ) 3.56 (8H, m), 6.68 (2H, d,  $J$  6.0 Hz), 6.92 (2H, d,  $J$  8.8 Hz), 7.79 (2H, d,  $J$  8.8 Hz), 8.31 (2H, d,  $J$  6.0 Hz), 9.80 (1H, s).

##### 3-Hydroxy-4-[4-(4-Pyridyl)Piperazino]Flavone

To a solution of 0.12 ml of 2-hydroxyacetophenone and 0.25 g of 4-[4-(4-pyridyl)piperazino]benzaldehyde in ethanol, 0.36 g of 70% KOH aq was added. The mixture was left, with stirring, for 1 week. Then, once again, 0.36 g of 70% KOH aq was added, and the mixture was treated with 0.7 ml of 30% hydrogen peroxide. After 4 hr, it was diluted with water, and the suspension was neutralized with diluted HCl. The precipitate was filtered and washed with water. It was crystallized from acetonitrile. Yield 25%; mp 264°C;  $^1\text{H}$  NMR (200 MHz,  $\text{CDCl}_3$ ) 3.54 (8H, m), 6.71 (2H, d,  $J$  6.4 Hz), 7.04 (2H, d,  $J$  9.1 Hz), 7.40 (1H, m), 7.57 (1H, d,  $J$  7.8), 7.68 (1H, m), 8.23 (2H, d,  $J$  9.1 Hz), 8.24 (1H, d,  $J$  9.5 Hz), 8.32 (2H, d,  $J$  6.4 Hz); MS (EI) m/z 399.1 ( $M^+$ ), 371.1, 342.1, 292.1, 264.0, 251.0, 237.0, 149.0, 106.0, 91.0, 69.1.

##### 4-[4-(3-Hydroxyflavonyl)Piperazino]-1-(3-Sulfopropyl)Pyridinium (PPZ)

A solution of 30 mg of 3-hydroxy-4-[4-(4-pyridyl)piperazino]flavone and 13  $\mu\text{l}$  of 1,3-propanesultone in 2 ml of dry DMF was heated at 100°C for 10 hr. The product was filtered and washed with DMF;

yield 90%; mp 270°C–275°C (decomp.); UV max in acetonitrile 380 nm,  $\epsilon = 30,000 \text{ l} \times \text{mol}^{-1} \times \text{cm}^{-1}$ ;  $^1\text{H}$  NMR (200 MHz,  $\text{CDCl}_3$ ) 2.11 (2H, m), 2.37 (2H, t,  $J$  7.0 Hz), 3.57 (4H, t,  $J$  5.6 Hz), 3.89 (4H, t,  $J$  5.6 Hz), 4.32 (2H, t,  $J$  6.7 Hz), 7.09 (2H, d,  $J$  9.0 Hz), 7.26 (2H, d,  $J$  7.4 Hz), 7.44 (1H, ddd,  $J$  8.2, 6.1, 1.8 Hz), 7.61 (1H, d,  $J$  8.4 Hz), 7.76 (1H, m), 8.09 (1H, d,  $J$  8.2 Hz), 8.16 (2H, d,  $J$  9.0), 8.35 (2H, d,  $J$  7.4 Hz); MS (FAB) m/z 522.0, 400.0, 232.

#### Preparation of Vesicles Samples and Fluorescence Measurements

For binding studies, large unilamellar vesicles (LUV) of DOPC (0.12  $\mu\text{m}$  in diameter) were used. They were obtained by the classical extrusion method as described previously [35]. LUVs were labeled by adding an aliquot (generally 1  $\mu\text{l}$ ) of probe stock solution (2 mM) in methanol (DMSO in the case of PPZ) to 2 ml solutions of vesicles in increasing concentrations (from 0 to 800  $\mu\text{M}$  in lipids). Preparation and labeling of EYPC and EYPG vesicles were performed applying the same procedures. The fluorescence intensities, corresponding to the integrated areas under the emission spectra, were determined immediately after the labeling for F, F2N8, and F4N1. In the case of PPZ, the intensity was recorded after 10 min, the time required to get a stable intensity. The fluorescence quantum yields of the probes embedded in a lipid environment were determined as previously described [36], the reference being 4'-diethylamino-3-hydroxyflavone with a quantum yield of 52% in ethanol [10].

For quenching experiments by the parallax method, lipid vesicles were prepared according to Kachel et al. [28] with small modifications. DOPC (85%) and nitroxide-labeled PCs (15%) were mixed in chloroform in order to obtain a final concentration of 400  $\mu\text{M}$ . The mixtures were dried under  $\text{N}_2$  and kept under vacuum for 30 min, and then resuspended in ethanol or in octylglucoside solution at 50 mM (120  $\mu\text{l}$ ) by continuous rotation using a rotary evaporator for 30 min. Finally, 6 ml of buffer (15 mM HEPES, pH 7.4) was added and vortexed briefly. The sizes of vesicles were determined by light scattering method using a N4SD Coultronics Nanosizer. The vesicles obtained by the ethanol dilution method were of the same size of LUV (0.12  $\mu\text{m}$ ), while those obtained with octylglucoside were somewhat larger (0.4  $\mu\text{m}$ ). The final concentration of the probes and the labeling procedure were the same as for the binding experiments.

#### Quenching Experiments and the Parallax Method

Fluorescence intensity of labeled vesicles, either DOPC or DOPC mixed with 15% nitroxide lipids, was measured in a 1 cm semimicro quartz cuvette as described in the subsection on binding studies. The measured fluorescence intensities, corresponding to the integrated areas under the emission spectra, were corrected for the background signal of the corresponding unlabeled vesicles. This background intensity was less than 4% of the measured intensity, except for PPZ (about 10%). The excitation wavelength was 400 nm and the excitation and emission slits were set at 4 nm (8 nm in the case of PPZ).

Using the corrected  $F/F_0$  values, the distance of the fluorophores from the center of the bilayer was calculated using the parallax equation as developed by London and collaborators [25, 26, 28, 37]:  $Z_{\text{cf}} = L_{\text{cl}} + [-\ln(F_1/F_2)/\pi C - L_{21}^2]/2L_{21}$ , where  $Z_{\text{cf}}$  is the distance of the fluorophore from the center of the bilayer,  $F_1$  and  $F_2$  are the fluorescence intensities in the presence of the shallow quencher (quencher 1) or the deeper quencher (quencher 2), respectively,  $L_{\text{cl}}$  is the distance of the shallow quencher from the center of the bilayer,  $L_{21}$  is the distance between the shallow and deep quenchers, and  $C$  the concentration of quencher in molecules/ $\text{\AA}^2$  (equals mole fraction of nitroxide-labeled phospholipid/area per phospholipid; presently  $C = 0.15/70 \text{ \AA}^2$  [32]). For a given chromophore, the quenching by the two most efficient quenchers (TempoPC/5-SLPC or 5-SLPC/12-SLPC; see Table 2) is used to calculate  $Z_{\text{cf}}$  [25]. The values used for the distances of the nitroxide group from the bilayer center were 5.85  $\text{\AA}$  for 12-SLPC, 12.15  $\text{\AA}$  for 5-SLPC, and 19.5  $\text{\AA}$  for TempoPC [25, 37].

Received: July 26, 2002

Revised: September 14, 2002

Accepted: September 18, 2002

#### References

- Emptage, N.J. (2001). Fluorescent imaging in living systems. *Curr. Opin. Pharmacol.* 1, 521–525.
- Harvath, L. (1999). Overview of fluorescence analysis with the confocal microscope. *Methods Mol. Biol.* 115, 149–158.
- So, P.T., Dong, C.Y., Masters, B.R., and Berland, K.M. (2000). Two-photon excitation fluorescence microscopy. *Annu. Rev. Biomed. Eng.* 2, 399–429.
- Demchenko, A.P., Klymchenko, A.S., Pivovarenko, V.G., and Ercelen, S. (2002). Ratiometric probes: design and application. In *Fluorescence Spectroscopy, Imaging and Probes - New Tools in Chemical, Physical and Life Sciences*, R. Kraayenhof, A.J.W.G. Visser, and H.C. Gerritsen, eds. (Heidelberg: Springer-Verlag). pp 101–110.
- Valeur, B. (2002). *Molecular Fluorescence: Principles and Applications* (Weinheim: Wiley-VCH).
- Loew, L.M. (1982). Design and characterization of electrochromic membrane probes. *J. Biochem. Biophys. Methods* 6, 243–260.
- De Silva, A.P., Gunaratne, H.Q.N., Gunnlaugsson, T., Huxley, A.J.M., McCoy, C.P., Rademacher, J.T., and Rice, T.E. (1997). Signaling recognition events with fluorescent sensors and switches. *Chem. Rev.* 97, 1515–1566.
- Sengupta, P.K., and Kasha, M. (1979). Excited state proton-transfer spectroscopy of 3-hydroxyflavone and quercetin. *Chem. Phys. Lett.* 68, 382–385.
- McMorrow, D., and Kasha, M. (1984). Intramolecular excited-state proton transfer in 3-hydroxyflavone. Hydrogen-bonding solvent perturbations. *J. Phys. Chem.* 88, 2235–2243.
- Chou, P.-T., Martinez, M.L., and Clements, J.-H. (1993). Reversal of excitation behavior of proton-transfer vs. charge-transfer by dielectric perturbation of electronic manifolds. *J. Phys. Chem.* 97, 2618–2622.
- Swinney, T.C., and Kelley, D.F. (1993). Proton transfer dynamics in substituted 3-hydroxyflavones: solvent polarization effects. *J. Chem. Phys.* 99, 211–221.
- Ormsom, S.M., Brown, R.G., Vollmer, F., and Rettig, W. (1994). Switching between charge- and proton-transfer emission in the excited state of a substituted 3-hydroxyflavone. *J. Photochem. Photobiol. A. Chem.* 81, 65–72.
- Sarkar, M., Ray, J.G., and Sengupta, P.K. (1996). Effect of reverse micelles on the intramolecular excited-state proton-transfer (ESIPT) and dual luminescence behavior of 3-hydroxyflavone. *Spectrochim. Acta A* 52, 275–278.
- Klymchenko, A.S., and Demchenko, A.P. (2002). Probing the aqueous and nonaqueous reverse micelles by 3-hydroxyflavone derivatives with two-color ratiometric response. *Langmuir* 18, 5637–5639.
- Bondar, O.P., Pivovarenko, V.G., and Rowe, E.S. (1998). Flavonols – new fluorescent membrane probes for studying the interdigitation of lipid bilayers. *Biochim. Biophys. Acta* 1369, 119–130.
- Dennison, S.M., Guharay, J., and Sengupta, P.K. (1999). Excited-state intramolecular proton transfer (ESIPT) and charge transfer (CT) fluorescence probe for model membranes. *Spectrochim. Acta A* 55, 1127–1132.
- Duportail, G., Klymchenko, A.S., Mely, Y., and Demchenko, A.P. (2001). New fluorescence probe with strong ratiometric response to surface charge of phospholipid membranes. *FEBS Lett.* 508, 196–200.
- Nemkovich, N.A., Kruchenok, J.V., Rubinov, A.N., Pivovarenko, V.G., and Baumann, W. (2001). Site-selectivity in excited-state intramolecular proton transfer in flavonols. *J. Photochem. Photobiol. A* 139, 53–62.
- Klymchenko, A.S., Ozturk, T., Pivovarenko, V.G., and Demchenko, A.P. (2001). 3-hydroxychromone with dramatically improved fluorescence properties. *Tetrahedron Lett.* 42, 7967–7970.
- Klymchenko, A.S., Ozturk, T., Pivovarenko, V.G., and Demchenko, A.P. (2002). Synthesis of furanochromones: a new step in improvement of fluorescence properties. *Tetrahedron Lett.* 43, 7079–7082.
- Kraayenhof, R., Sterk, G.J., and Wong Fong Sang, H.W. (1993).

- Probing biomembrane interface potential and pH profiles with a new type of float-like fluorophores positioned at varying distance from the membrane surface. *Biochemistry* 32, 10057–10066.
- 22. Epand, R.M., and Kraayenhof, R. (1999). Fluorescent probes used to monitor membrane interfacial polarity. *Chem. Phys. Lipids* 101, 57–64.
  - 23. Smith, M.A., Neumann, R.M., and Webb, R.A. (1968). A modification of the Algar-Flynn-Oyamada preparation of flavonols. *J. Heterocycl. Chem.* 5, 425–426.
  - 24. Klymchenko, A.S., and Demchenko, A.P. (2002). Electrochromic modulation of excited-state intramolecular proton transfer: the new principle in design of fluorescence sensors. *J. Am. Chem. Soc.* 124, 12372–12379.
  - 25. Chattopadhyay, A., and London, E. (1987). Parallax method for direct measurement of membrane penetration depth utilizing fluorescence quenching by spin-labeled phospholipids. *Biochemistry* 26, 39–45.
  - 26. Abrams, F.S., and London, E. (1993). Extension of parallax analysis of membrane penetration depth in the polar region of model membranes. Use of fluorescence quenching by a spin-label attached the phospholipids polar headgroup. *Biochemistry* 32, 10826–10831.
  - 27. Wiener, M.C., and White, S.H. (1992). Structure of a fluid dioleoylphosphatidylcholine bilayer determined by joint refinement of x-ray and neutron diffraction data. III Complete structure. *Biophys. J.* 61, 434–447.
  - 28. Kachel, K., Asuncion-Punzalan, E., and London, E. (1998). The location of fluorescence probes with charged groups in model membranes. *Biochim. Biophys. Acta* 1374, 63–76.
  - 29. Asuncion-Punzalan, E., and London, E. (1995). Control of the depth of molecules within membranes by polar groups: determination of the location of anthracene-labeled probes in model membranes by parallax analysis of nitroxide-labeled phospholipids induced fluorescence quenching. *Biochemistry* 34, 11460–11466.
  - 30. Hubner, W., and Blume, A. (1998). Interactions at the lipid-water interface. *Chem. Phys. Lipids* 96, 99–123.
  - 31. Langner, M., and Kubica, K. (1999). The electrostatics of the lipid surfaces. *Chem. Phys. Lipids* 101, 3–35.
  - 32. Tielemans, D.P., Marrink, S.J., and Berendsen, H.J.C. (1997). A computer perspective of membranes: molecular dynamic studies of lipid bilayer systems. *Biochim. Biophys. Acta* 1331, 235–270.
  - 33. Pasenkiewicz-Gierula, M., Takaoka, Y., Miyagawa, H., Kitamura, K., and Kusumi, A. (1997). Hydrogen bonding of water to phosphatidylcholine in the membrane as studied by a molecular dynamics simulation: location, geometry, and lipid-lipid bridging via hydrogen-bonded water. *J. Phys. Chem. A.* 101, 3677–3691.
  - 34. Mashl, R.J., Scott, H.L., Subramaniam, S., and Jacobsson, E. (2001). Molecular simulation of dioleoylphosphatidylcholine lipid bilayers at differing levels of hydration. *Biophys. J.* 81, 3005–3015.
  - 35. Lières, D., Dauty, E., Behr, J.-P., Mély, Y., and Duportail, G. (2001). DNA condensation by an oxidizable cationic detergent. Interactions with lipid vesicles. *Chem. Phys. Lipids* 111, 59–71.
  - 36. Demas, G.A., and Crossby, J.N. (1971). Measurement of photoluminescence quantum yields. *J. Phys. Chem.* 75, 991–1024.
  - 37. Kaiser, R.D., and London, E. (1998). Location of diphenylhexatriene (DPH) and its derivatives within membranes: comparison of different fluorescence quenching analyses of membrane lipids. *Biochemistry* 37, 8180–8190.